Int. J. Solids Structures Vol. 30, No. 6, pp. 767–777, 1993
Printed in Great Britain

0020–7683/93 $6.00+ .00
Pergamon Press Ltd

ASYMPTOTIC INTERFACE CORNER SOLUTIONS FOR BUTT TENSILE JOINTS

E. D. REEDY, JR
Sandia National Laboratories, Albuquerque, NM 87185, U.S.A.

(*Received* 1 *April* 1992; *in revised form* 1 *September* 1992)

Abstract—In previous work, the intensity of the stress singularity of type r^{δ} ($\delta < 0$) found at the interface corner between a thin elastic adhesive layer and one of a pair of rigid adherends was fully determined for a butt tensile joint. This stress intensity factor, referred to here as the free-edge stress intensity factor K_f, can be applied to both plane strain and axisymmetric geometries. This study investigates the potential application of a K_f-based failure criterion to butt tensile joints. Detailed elastic–plastic finite element calculations for adhesive properties representative of a high strength epoxy indicate that when residual cure stress can be neglected (1) the region dominated by the interface corner singularity is reasonably large relative to adhesive layer thickness, (2) the plastic yield zone is contained within the singular field at nominal failure loads, and (3) the plastic zone size is characterized by K_f and displays the expected load level and layer thickness dependence. The way uniform adhesive shrinkage (thermal contraction) during cure alters interface corner stress fields is also discussed. When adhesive shrinkage is present, both constant and singular terms must be included in the asymptotic solution to get good agreement with full field finite element results. In general, there is no unique relation between the size of the interface corner yield zone and K_f, although for a prescribed shrinkage strain, K_f does characterize the extent of plastic yielding. Calculated results suggest that the presence of residual stress can have a considerable effect on the relation between bond thickness and joint strength.

INTRODUCTION

Within the context of elasticity theory, a stress singularity of type Kr^{δ} ($\delta < 0$) can exist at an interface corner (e.g. the point where an interface between bonded materials intersects a stress-free edge) (Williams, 1952). The magnitude of the stress intensity factor K characterizes the stress state in the region of the interface corner. Several experimental studies have investigated the use of an interface corner stress intensity factor to predict the failure of bonded materials. Gradin (1982) tested three different types of 3 layer, steel/epoxy/steel model laminates subjected to various loading conditions. Groth (1988) tested single-lap joints with a spew fillet for a range of overlap lengths. Hattori *et al.* (1989) molded epoxy models with small Fe–Ni inserts to investigate failure as a molding cools. The data reported in these three studies lend support to an interface corner K-based failure analysis.

In recent work, a relation defining the interface corner stress intensity factor for the idealized case of a thin linear elastic adhesive layer bonded to rigid adherends (e.g. $L/h > 20$, Fig. 1) and subjected to either transverse tension or uniform adhesive shrinkage has been fully determined for plane strain and axisymmeric geometries (Reedy, 1990, 1991). This stress intensity factor, referred to here as the free-edge stress intensity factor K_f, is applicable when the adherends are much stiffer than the adhesive; as is the case of steel adherends and epoxy adhesive. The geometry considered models adhesive butt tensile test configurations that bond a thin adhesive layer between two relatively rigid metal cylinders (e.g. ASTM D897-78 and D2095-72, 1990 Annual Book of ASTM Standards, Volume 15.06

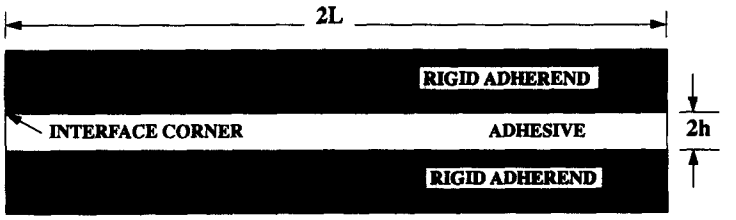

Fig. 1. Idealized butt tensile joint geometry.

Ahesives). K_f was determined by a technique that combines results of an asymptotic stress singularity analysis with those of a detailed finite element analysis.

To be useful as a failure criterion, the stress state characterized by K_f must dominate a region about the interface corner that is significantly larger than the fracture process zone, intrinsic flaw size and the plastic yield zone. Here, attention is focused on the size of the plastic yield zone since it presumably contains the fracture process zone. Results illustrating the nature of the plastic yield zone at an interface corner have been previously reported by Chen and Sun (1986), and Groth and Brottare (1988) have examined the plastic yield zone in a butt joint with a thick adhesive layer. In the following, results of detailed elastic–plastic finite element analyses of a thin adhesive layer with negligible cure shrinkage and with properties representative of a high strength epoxy are presented that (1) establish the region dominated by the interface corner stress singularity, (2) examine the extent and nature of adhesive yielding at nominal bond failure loads, and (3) determine the capacity of K_f to characterize the extent of yielding. In addition, the effect of adhesive shrinkage (thermal contraction) during cure on calculated interface corner stress distributions is discussed.

K_f RELATION

The K_f relation for a thin linear elastic layer bonded to rigid adherends and subjected to transverse tension or uniform adhesive shrinkage has been determined by Reedy (1990, 1991), and takes the form

$$K_f = \sigma^* h^{1-\lambda} A_p(\nu), \tag{1}$$

where σ^* is a characteristic stress, $2h$ is layer thickness, $\lambda - 1$ is the order of the stress singularity, and $A_p(\nu)$ is a function defined for loadings that can be obtained by superimposing the solution for a uniform pressure applied to the layer's exterior edge and a uniform stress state. $A_p(\nu)$ and λ are functions of Poisson's ratio ν only, and their values are listed in Table 1. Note that the characteristic stress σ^* is the in-plane stress found at the center of the layer in a region remote from the stress-free edge. The characteristic stress associated with a nominal applied transverse (butt tensile) stress σ_t^* and associated strain ε_t^* for a material with Young's modulus E is

$$\sigma^* = \left(\frac{\nu}{1-\nu}\right)\sigma_t^* = \frac{\nu E \varepsilon_t^*}{(1+\nu)(1-2\nu)}, \tag{2}$$

while that for uniform adhesive shrinkage ε_0^* (e.g. $\varepsilon_0^* = \alpha \Delta T$ for a material with thermal expansion coefficient α subjected to a uniform temperature change ΔT) is given by

$$\sigma^* = -\frac{E\varepsilon_0^*}{(1-\nu)}. \tag{3}$$

Table 1. Calculated dependence of the order of the interface corner stress singularity ($\lambda - 1$) and function $A_p(\nu)$ on Poisson's ratio ν

ν	$\lambda - 1$	$A_p(\nu)$
0.05	−0.0774	14.700
0.10	−0.1330	6.630
0.15	−0.1788	3.960
0.20	−0.2189	2.630
0.25	−0.2553	1.840
0.30	−0.2888	1.320
0.35	−0.3203	0.948
0.40	−0.3501	0.654
0.45	−0.3784	0.391
0.49	−0.4001	0.150

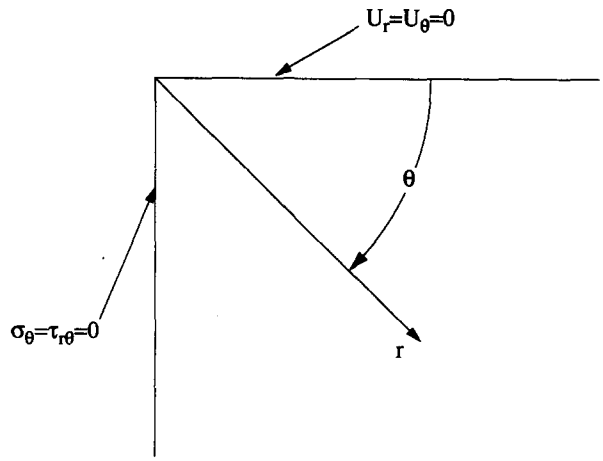

Fig. 2. Coordinate system in region of interface corner. Note: the stress-free edge is at $\theta = -\pi/2$.

K_f is defined so that the stress component normal to the interface $\sigma_\theta(r, 0) = K_f r^{\lambda-1}$ (coordinate system defined in Fig. 2). Stress components in the region dominated by the stress singularity take the form

$$\sigma_r = K_f r^{\lambda-1} f_r(\theta), \tag{4}$$

$$\sigma_\theta = K_f r^{\lambda-1} f_\theta(\theta), \tag{5}$$

$$\sigma_{r\theta} = K_f r^{\lambda-1} f_{r\theta}(\theta). \tag{6}$$

Functions $f_r(\theta)$, $f_\theta(\theta)$ and $f_{r\theta}(\theta)$ depend on ν, and are fully determined by the asymptotic singularity analysis, however, since they are rather lengthy they will not be listed (see Table 2 for selected $\nu = 0.4$ values). For the plane strain condition considered here, out-of-plane stress $\sigma_z = \nu(\sigma_r+\sigma_\theta)$, mean stress $\sigma_m = (\sigma_r+\sigma_\theta+\sigma_z)/3$, and effective stress $\sigma_e = (3J_2)^{1/2}$ (J_2 is the second stress deviator invariant).

ANALYSIS

Detailed plane strain finite element calculations were carried out to provide full field, elastic–plastic solutions for the idealized butt tensile geometry shown in Fig. 1. The adhesive layer has thickness $2h$, and length $2L$, with results presented for $h = 0.125$ and 0.250 mm. Preliminary calculations showed that the stress state at the center of the layer is uniform for $L/h = 20$. All results reported here are for $L/h = 20$, and apply to L/h values of 20 or greater (the layer behaves like a semi-infinte layer with h as the only finite length scale). One quarter of the layer was modeled with boundary conditions consistent with attachment

Table 2. Selected values of functions defining angular dependence of stress components in region dominated by stress singularity ($\nu = 0.4$)

$\theta =$	0	$-\pi/6$	$-\pi/4$	$-\pi/3$	$-\pi/2$
$f_r(\theta) =$	0.667	0.947	1.078	1.158	1.075
$f_\theta(\theta) =$	1.000	0.572	0.346	0.160	0.000
$f_{r\theta}(\theta) =$	−0.397	−0.541	−0.488	−0.362	0.000

to a rigid surface and symmetric loading (Fig. 3). Calculations were carried out for a butt tensile loading enforced by displacing the layer's lower edge relative to the upper edge. Figure 3 shows a typical finite element mesh ($h = 0.125$ mm). Since the object of this analysis is to provide full field solutions to compare with interface corner asymptotic results, the mesh is highly refined in the region of the interface corner. There are 24 rings of elements surrounding the interface corner with radial nodal positions at $r = 0$, 0.033, 0.067, 0.100 $(10^{0.125i})/10$ μm, where $i = 1, 2, \ldots, 21$. The finite element calculations were performed with the ABAQUS (1989) code using 4 node bilinear elements. The mesh shown in Fig. 3 contains 876 elements and has 1930 degrees of freedom.

Results are presented for adhesive properties representative of a high strength epoxy. The adhesive is modeled as elastic–perfectly plastic with Young's modulus $E = 2500$ MPa, Poisson's ratio $v = 0.4$, and yield strength $\sigma_y = 55$ MPa. The butt tensile strength for a typical epoxy adhesive with a $2h = 0.25$ mm thick bond is approximately 50 MPa (Guess, 1991). Note, an applied nominal butt tensile strain of 1% (i.e. $\varepsilon_t^* = 0.01$) is associated with a nominal applied transverse stress σ_t^* of 53.6 MPa [see eqn (2)]. All results reported below are based upon these material properties. The finite element analysis uses a standard plasticity model with a von Mises yield surface and associated plastic flow rule.

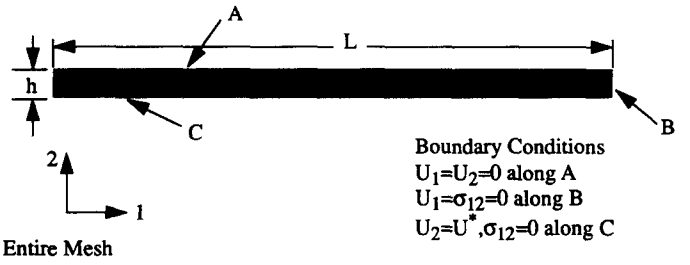

Entire Mesh

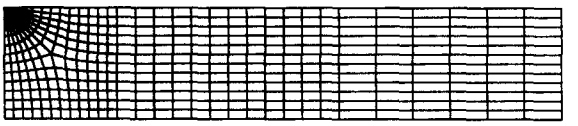

Detail of mesh near free edge.

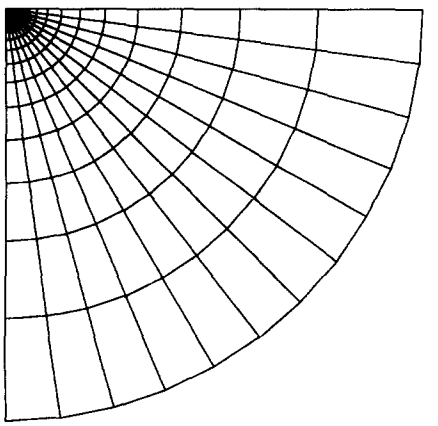

Detail of mesh near interface corner. There are 24 element rings.

Fig. 3. Typical finite element mesh used in analysis.

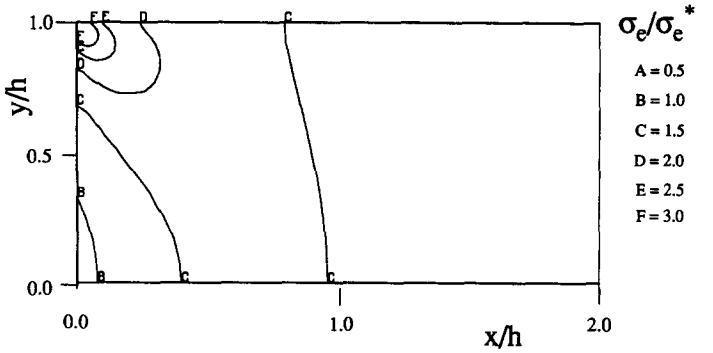

Fig. 4. Effective stress contours for a butt tensile loading (linear elastic solution).

RESULTS AND DISCUSSION

The first three parts of the following section apply to a condition of negligible residual fabrication stress. The effect of residual stress generated by uniform adhesive shrinkage (thermal contraction) during cure on interface corner stress fields is addressed in the final part.

Region dominated by interface corner singularity

Figures 4 and 5 plot linear elastic finite element results that portray the nature of the interface corner stress field for an adhesive layer subjected to the butt tensile loading defined in Fig. 3. Effective stress contours normalized with respect to σ_e^*, the nominal effective stress found at the center of the adhesive layer in a region remote from the stress-free edge, are plotted in Fig. 4. Effective stress decreases monotonically with distance from the interface corner, with a large region of the adhesive subjected to an effective stress greater than the nominal value σ_e^*. Effective stress values are quite high in the region surrounding the interface corner (for $r/h < 0.2$, $\sigma_e/\sigma_e^* > 2$), and $\sigma_e/\sigma_e^* \sim 1$ only when $r/h > 4$. These results suggest that plastic yielding will occur first in the region of the interface corner at load levels well below that required to fully yield the adhesive layer. One might speculate that small, pre-existing flaws grow in the highly deformed interface corner yield zone to initiate cohesive failure.

Mean stress contours normalized with respect to σ_m^*, the nominal mean stress found at the center of the adhesive layer, are plotted in Fig. 5. The region of elevated mean stress is quite localized, $\sigma_m/\sigma_m^* > 1$ only when $r/h < 0.1$. Furthermore, mean stress does not decrease monotonically with distance from the interface corner. For example, along the interface, the mean stress initially decreases with distance until at $r/h = 0.5$, $\sigma_m/\sigma_m^* < 0.7$; mean stress then increases to its nominal value σ_m^* at $r/h \sim 4$. Elevated values of interfacial mean stress are associated with high peel stress, and peel stress is presumably associated

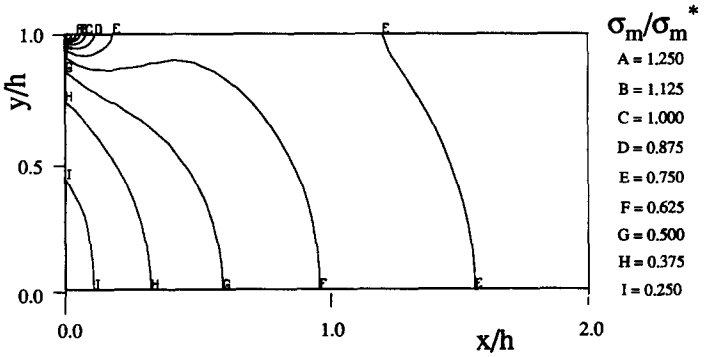

Fig. 5. Mean stress contours for a butt tensile loading (linear elastic solution).

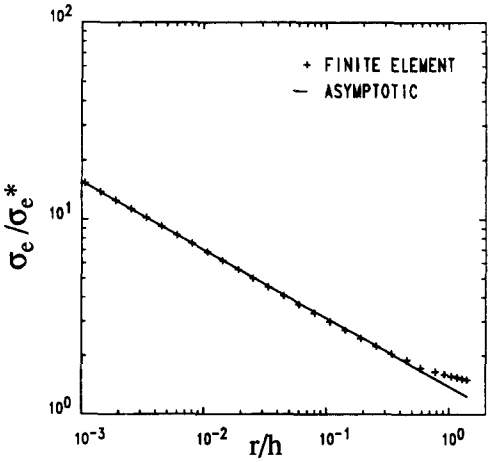

Fig. 6. Comparison of linear elastic finite element and asymptotic singular solutions for effective stress along $\theta = -\pi/4$.

with adhesive failure of the interfacial bond. However, the rather small size of the region of elevated mean stress does raise the question as to its role in the failure process.

The region dominated by the interface corner stress singularity can be estimated by comparing the full field finite element solution with the singular asymptotic stress field defined by eqns (4)–(6). Figure 6 compares linear elastic finite element and asymptotic solutions for effective stress along the ray bisecting the interface corner region ($\theta = -\pi/4$), while Fig. 7 compares results for mean stress along the interface ($\theta = 0$). Asymptotic and finite element results for effective stress are in excellent agreement for $r/h < 0.6$, and differ by only 15% at $r/h = 1.0$ (Fig. 6). This result clearly suggests that the singular asymptotic solution for effective stress does dominate a large region. The comparison of interfacial mean stress shows that the asymptotic and full field finite element solutions are in excellent agreement for $r/h < 0.3$. The finite element and asymptotic solutions begin to diverge for $r/h > 0.5$ as mean stress attains its minimum value and then increases to the stress level σ_m^* found at the center of the layer.

Extent and nature of adhesive yielding

Elastic–plastic finite element results for a butt tensile joint with $h = 0.125$ mm indicate that a finger-like plastic yield zone grows in a self-similar manner from the interface corner

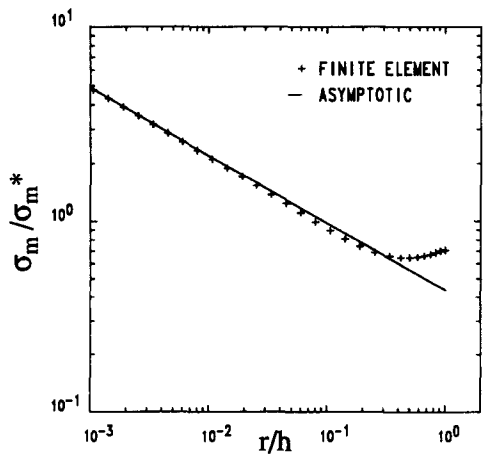

Fig. 7. Comparison of linear elastic finite element and asymptotic singular solutions for mean stress along the interface, $\theta = 0$.

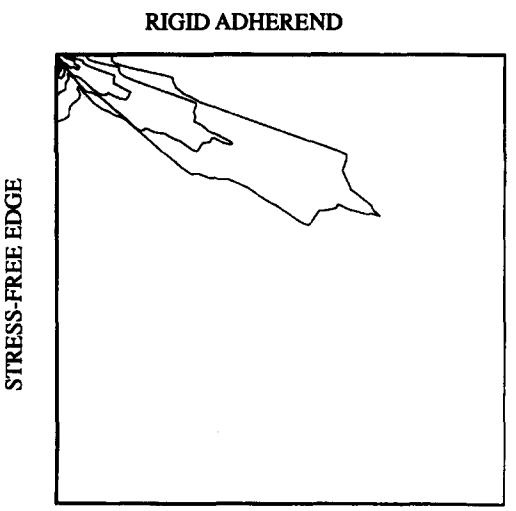

Fig. 8. Growth of plastic yield zone with butt tensile load. A 0.02×0.02 mm region at the interface corner of a 0.25 mm thick bond shown for nominal bond strains $\varepsilon_t^* = 0.004$, 0.006, 0.008 and 0.010.

at roughly 30° ($\theta = -\pi/6$) from the interface. Figure 8 plots the yield zone boundary for $\varepsilon_t^* = 0.004$, 0.006, 0.008 and 0.010 (recall, the nominal adhesive butt tensile strength for a $2h = 0.250$ mm thick epoxy bond is roughly 50 MPa, which corresponds to a nominal applied transverse strain ε_t^* equal to 0.010). The length of the yield zone r_p, defined as its maximum radial extent, increases rapidly with load. When ε_t^* is increased from 0.005 to 0.010, r_p/h increases from 0.02 to 0.15. Even at the relatively high load level $\varepsilon_t^* = 0.010$, the size of the yield is significantly smaller than the region $r/h < 0.6$ dominated by the singular asymptotic solution for effective stress (see previous section).

Capacity of K_f to characterize adhesive yielding

Elastic–plastic finite element results are used to establish how the yield zone grows with increasing K_f. The length r_p of the finger-like interface corner yield zone shown in Fig. 8 is defined as its maximum radial extent. Figure 9 plots calculated r_p versus the associated K_f value defined by eqns (1) and (2). Plotted results are for loads of up to $\varepsilon_t^* = 0.010$ (corresponding to the nominal adhesive butt tensile strength), and adhesive thickness $h = 0.125$ and 0.250 mm. The log–log plot of r_p versus K_f collapses the finite element results

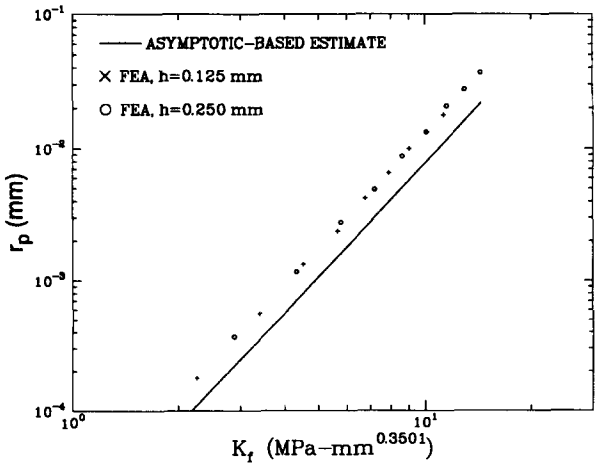

Fig. 9. Length of plastic yield zone versus associated free-edge stress intensity factor. Elastic–plastic finite element results are compared with lower bound asymptotic-based estimate.

for the two different adhesive thicknesses to a single straight line with a slope (least square fit) of 2.9 mm MPa^{-1} $mm^{-0.3501}$.

The linear elastic, interface corner singularity solution can be used to develop a lower bound estimate for the size of the yield zone. First note, effective stress in the region dominated by the stress singularity can be expressed (substitute eqns (4)–(6) in the definition of effective stress) as

$$\sigma_e = K_f r^{\lambda-1} f_e(\theta), \tag{7}$$

where $f_e(\theta)$ depends on the functions $f_r(\theta)$, $f_\theta(\theta)$ and $f_{r\theta}(\theta)$. Equation (7) is solved for the radius where effective stress equals adhesive yield strength σ_y, and this radius is taken as the estimate for r_p:

$$r_p = CK_f^{1/(1-\lambda)}, \tag{8}$$

where

$$C = (\sigma_y/f_e(\theta))^{1/(\lambda-1)}. \tag{9}$$

Since the elastic–plastic finite element solution indicates maximum yielding at $\theta = -\pi/6$ (Fig. 8), $\theta = -\pi/6$ is used in eqn (9) (note, for $\nu = 0.4$, $f_e(-\pi/6) = 1.004$). A relation similar to eqn (8) was used by Groth and Brottare (1988) in their study of yielding in butt joints with a thick adhesive layer, but their relation is based on the radial stress component along the free edge. Figure 9 shows that a log–log plot of the asymptotic-based r_p estimate [eqn (8)] produces a straight line parallel to the finite element results (slopes of the two lines are within 1%). The value of C as defined by eqn (9) is 1.1×10^{-5} $MPa^{-2.9}$ while a least square fit of the finite element results plotted in Fig. 9 suggest a value of 1.7×10^{-5} $MPa^{-2.9}$. The smaller C value reflects the lower bound nature of the asymptotic-based r_p estimate. The r_p estimate is based on a linear elastic solution, and does not take into account the redistribution of stress in the region of the interface corner. Note that the analogous crack-tip yield zone estimate, based on the linear elastic crack-tip stress field, is typically taken to be twice the radius where $\sigma_e = \sigma_y$ (Kanninen, 1985).

The results plotted in Fig. 9 clearly show that K_f characterizes r_p for material properties, adhesive thicknesses, and load levels of practical interest. The relation between K_f and r_p is expected to hold as long as the yield zone is sufficiently small compared to the K_f dominated region.

Effect of residual stress

Residual stress can be introduced into an adhesive bond during cool down from an elevated temperature curve. For example, the coefficient of thermal expansion α of an adhesive is roughly 50×10^{-6} °C^{-1}, and a 100°C cool down causes a shrinkage strain $\varepsilon_0^* = -0.005$. Figure 10 compares linear elastic finite element and singular asymptotic solutions for effective stress along the line bisecting the interface corner region ($\theta = -\pi/4$) when uniform adhesive shrinkage ε_0^* occurs (note, there is no applied transverse butt tensile strain, i.e. $\varepsilon_t^* = 0.00$). There is a marked difference in the two solutions. Agreement is improved considerably when the asymptotic solution includes constant as well as singular terms. The constant stress field that satisfies interface corner boundary conditions (Fig. 2) in the presence of uniform adhesive shrinkage ε_0^* has only one nonzero stress component, transverse stress σ_t^0. This is the only nonzero constant term associated with the asymptotic solution for uniform adhesive shrinkage, and

$$\sigma_t^0 = \frac{E\varepsilon_0^*}{\nu}. \tag{10}$$

As an aside, there are no nonzero constant terms associated with the asymptotic solution for a butt tensile loading. Figure 10 shows that asymptotic and linear finite element solutions

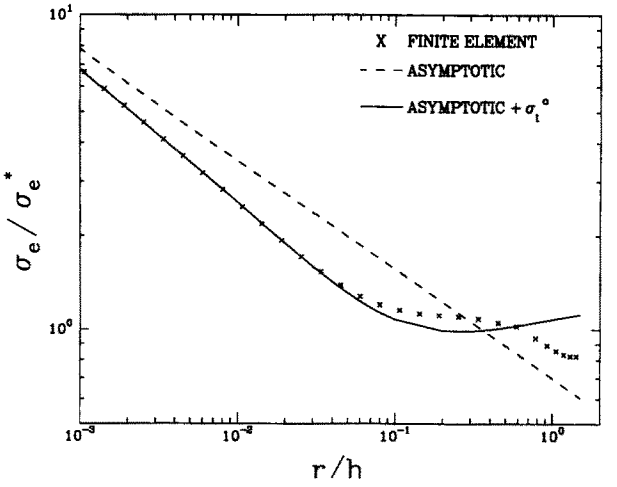

Fig. 10. Comparison of linear elastic finite element and asymptotic solutions for effective stress along $\theta = -\pi/4$ for an adhesive layer subjected to a uniform shrinkage strain ε_0^*.

are in good agreement with $r/h = 0.6$ when the asymptotic solution includes both singular and constant terms. Finite element calculations were carried out for several different values of ν to confirm eqn (10).

Yield zone extension during butt tensile loading is altered by the presence of adhesive shrinkage. Elastic–plastic finite element results are presented for an initial uniform adhesive shrinkage $\varepsilon_0^* = -0.0025$, with a maximum applied nominal butt tensile strain ε_t^* level of 0.01, and adhesive thickness $h = 0.125$ and 0.250 mm. Figure 11 plots calculated plastic zone size r_p versus the associated K_f value. Note, K_f depends on both ε_0^* and ε_t^* [the sum of the σ^* values calculated using eqns (2) and (3) is used in eqn (1)]. As in Fig. 9, a log–log plot of r_p versus K_f collapses the finite element results for the two different adhesive thicknesses to a single straight line with slope 2.9 mm MPa^{-1} $mm^{-0.3501}$. A comparison of Figs 9 and 11 shows that the finite element results for uniform adhesive shrinkage $\varepsilon_0^* = 0.0025$ are shifted parallel and to the right of results for the case of no shrinkage (i.e. when $\varepsilon_0^* = 0.00$). For a specified K_f value, the length of the plastic yield zone for a uniform adhesive shrinkage $\varepsilon_0^* = -0.0025$ is 60% of that for no shrinkage.

The previously derived asymptotic-based estimate for r_p [eqn (8)] considered only the singular stress field. This estimate uniquely relates r_p and K_f values, and does not display the observed ε_0^* dependence. An estimate based on the singular term plus the constant σ_t^0

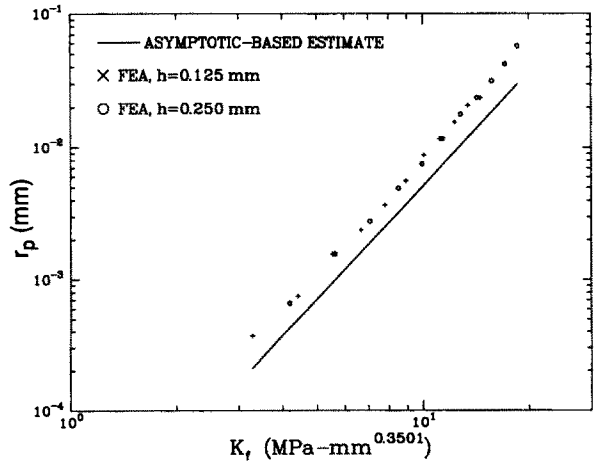

Fig. 11. Length of plastic yield zone versus associated free-edge stress intensity factor for an adhesive layer subjected to a uniform shrinkage strain $\varepsilon_0^* = -0.0025$ prior to butt tensile loading.

Table 3. Selected values of function $f(\varepsilon_0^*, \nu, \sigma_y/E)$

ε_0^*	0.000	−0.001	−0.002	−0.003	−0.004	−0.005
$f(\varepsilon_0^*, 0.4, 0.022)$	1.00	0.83	0.71	0.62	0.56	0.52

term associated with uniform adhesive shrinkage does reproduce the observed behavior. This estimate for r_p is derived in the same manner as used to derive eqn (8) with the exception that σ_t^0 is transformed to polar coordinates and added to the appropriate stress component defined in eqns (4)–(6). The modified r_p relation can be expressed as

$$r_p = CK_f^{1/(1-\lambda)} f\left(\varepsilon_0^*, \nu, \frac{\sigma_y}{E}\right). \tag{11}$$

As before, r_p is defined for $\theta = -\pi/6$. Table 3 lists selected f values for the same typical adhesive properties used in all the other calculations. For a fixed uniform adhesive shrinkage ε_0^*, the function f simply scales the eqn (8) plastic zone size estimate, and eqn (11) reduces eqn (8) when there is no adhesive shrinkage (i.e. when $\varepsilon_0^* = 0.00$). A comparison of Figs 9 and 11 shows that like the finite element results, the eqn (11) estimate for a uniform adhesive shrinkage $\varepsilon_0^* = -0.0025$ is shifted parallel and to the right of the estimate for the case of no adhesive shrinkage. When $\varepsilon_0^* = -0.0025$, the scale factor applied to r_p values for the case of no shrinkage is 0.66. This scale factor is nearly the same as that deduced by the elastic–plastic finite element analysis. To summarize, the modified asymptotic-based r_p estimate [eqn (11)] should be used when adhesive shrinkage ε_0^* occurs. The length of the interface corner yield zone is not uniquely related to a specific K_f value when adhesive shrinkage occurs. However, for a prescribed uniform shrinkage strain ε_0^*, r_p is fully characterized by the associated K_f value. This result suggests that if an adhesive fails at a critical K_f value, that value applies only to that adhesive when it is cured the same way (i.e. has the same ε_0^*).

Finally, note that if adhesive failure were to occur when r_p reaches a critical value (assuming intrinsic adhesive properties do not depend on method of cure, i.e. on ε_0^* value), then eqn (11) can be solved for the butt tensile strength (σ_t^*) for a prescribed adhesive shrinkage ε_0^* and layer thickness $2h$. Figure 12 plots such results for three values of ε_0^* assuming failure occurs when $r_p = 0.010$ mm (this choice is consistent with a 0.250 mm thick bond with no adhesive shrinkage failing at 52 MPa). The predicted adhesive butt tensile strength is a strong function of both layer thickness and adhesive shrinkage. These results suggest that the adhesive's apparent butt tensile strength increases as adhesive thickness decreases, and when adhesive shrinkage is minimized. Published butt tensile joint

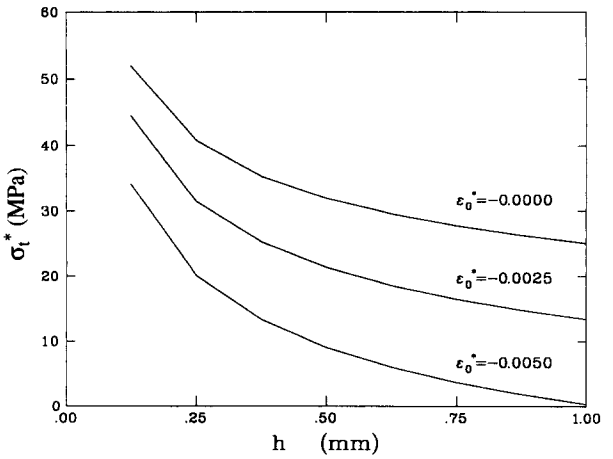

Fig. 12. Estimated butt tensile strength versus adhesive layer thickness for three values of adhesive shrinkage (assumed failure occurs when asymptotic-based r_p estimate equals 0.010 mm).

data do indeed indicate that joint strength increases with decreasing adhesive thickness (Anderson and DeVries, 1989).

CONCLUSIONS

An idealized butt tensile joint with rigid adherends and a thin adhesive bond layer was analysed. Linear elastic, asymptotic solutions for the interface corner stress field were compared with full field, elastic–plastic finite element results. The major findings of this study include:

—The interface corner stress singularity dominates a reasonably large region relative to layer thickness when residual cure stress can be neglected.
—When adhesive shrinkage (thermal contraction) is present, the asymptotic solution accurately represents the interface corner stress field over a significant region only when both constant and singular terms are included.
—Elastic–plastic finite element analysis reveals that a finger-like plastic zone grows from the interface corner. The yield zone is contained within the asymptotic field at nominal failure loads.
—For a prescribed shrinkage strain, the interface corner plastic yield zone is characterized by K_f, and it displays the expected load level and layer thickness dependence.
—Calculated results suggest that the presence of residual shrinkage stress has a significant effect on the relation between butt tensile strength and bond thickness.

Results of the present study support the possible use of a K_f-based failure criterion for butt tensile joints provided that the interface corner yield zone is sufficiently small at bond failure relative to the region accurately represented by the asymptotic, interface corner stress solution. However, one must recognize several potential difficulties that might arise when this approach is applied to real adhesives. First, most adhesives contain fillers and at least some porosity. One might expect a K_f-based failure criterion to fail if fillers and voids are not small relative to the region dominated by the asymptotic solution. Furthermore, it has been assumed that failure occurs with little or no stable flaw growth. Nevertheless, if stable flaw growth did occur, K_f might still prove useful in characterizing initial damage threshold limits. Those circumstances, if any, where a K_f-based failure criterion might apply can only be established by a careful experimental program.

Acknowledgement—This work was performed at Sandia National Laboratories and supported by U.S. Department of Energy under Contract DE-AC04-76DP00789.

REFERENCES

ABAQUS Version 4.8 (1989). Hibbitt, Karlsson and Sorensen, Inc., Providence, Rhode Island.
Anderson, G. P. and DeVries, K. L. (1989). Predicting strength of adhesive joints from test results. *Int. J. Fract.* **39,** 191–200.
Chen, J. K. and Sun, C. T. (1986). Elasto–plastic analysis of layered media with dissimilar materials. *Engng Fract. Mech.* **25,** 349–360.
Gradin, P. A. (1982). A fracture criterion for edge-bonded bimaterial bodies. *J. Compos. Mater.* **16,** 448–456.
Groth, H. L. (1988). Stress singularities and fracture at interface corners in bonded joints. *Int. J. Adhesion Adhesives* **8,** 107–113.
Groth, H. L. and Brottare, I. (1988). Evaluation of singular intensity factors in elastic–plastic materials. *J. Testing and Evaluation* **16,** 291–297.
Guess, T. R. (1991). Sandia National Laboratories, Albuquerque, NM, personal communication.
Hattori, T., Sakata, S. and Murakami, G. (1989). A stress singularity parameter approach for evaluating the interfacial reliability of plastic encapsulated LSI devices. *Trans. ASME, J. Electronic Packaging* **111,** 243–248.
Kanninen, M. F. and Popelar, C. H. (1985). *Advanced Fracture Mechanics*. Oxford University Press, New York.
Reedy, Jr, E. D. (1990). Intensity of the stress singularity at the interface corner between a bonded elastic and rigid layer. *Engng Fract. Mech.* **36,** 575–583.
Reedy, Jr, E. D. (1991). Intensity of the stress singularity at the interface corner of a bonded elastic layer subjected to shear. *Engng Fract. Mech.* **38,** 273–281.
Williams, M. L. (1952). Stress singularities resulting from various boundary conditions in angular corners of plates in extension. *Trans. ASME, J. Appl. Mech.* **74,** 526–528.